

## Pressure-induced phase transitions in cobalt-filled multiwalled carbon nanotubes

S. Karmakar,<sup>1</sup> Pawan K. Tyagi,<sup>2</sup> D. S. Misra,<sup>2</sup> and Surinder M. Sharma<sup>1</sup>

<sup>1</sup>*Synchrotron Radiation Section, Bhabha Atomic Research Centre, Mumbai 400 085 India*

<sup>2</sup>*Department of Physics, Indian Institute of Technology, Mumbai 400 076 India*

(Received 21 March 2006; published 22 May 2006)

High-pressure structural properties of cobalt nanowires encapsulated in multiwalled carbon nanotubes have been investigated up to a pressure of  $\sim 38$  GPa at room temperature. Our x-ray diffraction measurements show that cobalt, which exists in the face-centered-cubic (fcc) phase at ambient conditions in the carbon nanotubes, transforms irreversibly to a hexagonal close-packed (hcp) structure at  $\sim 9$  GPa. In comparison with the bulk Co, the compressibility of the fcc phase in nanowires is found to be similar to that of the high-pressure fcc phase [Phys. Rev. Lett. **84**, 4132 (2000)] and the hcp phase is slightly less compressible than the bulk. Multiwalled carbon nanotubes that encapsulate the cobalt nanowires do not undergo any other structural transformation with pressure except partial reversible amorphization beyond 9 GPa.

DOI: [10.1103/PhysRevB.73.184119](https://doi.org/10.1103/PhysRevB.73.184119)

PACS number(s): 61.46.-w

### INTRODUCTION

Carbon nanotubes show fascinating properties such as high strength, discrete electronic states, and structural helicity, etc., for which these are usefully employed in miniature devices, e.g., scanning probes,<sup>1</sup> electronic transistors,<sup>2,3</sup> field-emitting devices,<sup>4,5</sup> in nanofluidic industry,<sup>6</sup> etc. Carbon nanotubes can also be filled with biological molecules, giving rise to the possibilities of applications in biotechnology.<sup>7</sup> Encapsulation of various metals in multiwalled carbon nanotubes (MWCNTs) provides opportunities to study the physical properties of nanowires and nanoparticles of these metals.<sup>6,8</sup> Magnetic metal nanowires, encapsulated inside multiwalled carbon nanotubes, constitute an active and attractive field of research,<sup>9</sup> as these are promising materials for use in nanodevices and in the magnetic storage industry. In addition, recently these are also being considered as potential candidates for spintronics.<sup>10</sup> In fact, materials, when encapsulated inside carbon nanotubes, show interesting physical and structural properties that could be much different than their bulk counterparts.<sup>11,12</sup>

Our previous high-pressure structural investigations on iron-filled carbon nanotubes showed several remarkable features of nanowires and the nanotubes.<sup>12</sup> High-pressure structural studies showed that the filled multiwalled carbon nanotubes, unlike pristine tubes, show sudden polygonization at a pressure at which the interfacial part of the nanowires ( $\text{Fe}_3\text{C}$ ) also underwent an isostructural phase transition. As both transitions occur at the same pressure, the transformation mechanism remained unclear. Also the compressibilities of both components of the nanowires, viz.  $\text{Fe}_3\text{C}$  and  $\alpha\text{-Fe}$ , are found to be enhanced. So to understand the driving force and the mechanism for these coincident phase transitions, it is necessary to undertake careful studies on MWCNTs filled with some other similar metals. Recently, single-crystalline cobalt nanowires (having an aspect ratio  $\sim 100$ ), encapsulated in MWCNTs, have been synthesized by microwave plasma chemical vapor deposition (MPCVD) technique.<sup>13</sup> At ambient conditions, facilitated by energy minimization, these cobalt nanowires are found to have face-centered-cubic (fcc) structure ( $\beta$  phase).<sup>13</sup> Moreover, unlike Fe-filled MWCNTs,

no interfacial carbide formation has been observed in these tubes.

At ambient conditions, bulk cobalt is ferromagnetic and exists in either the stable hcp phase or the metastable (quenched) fcc phase.<sup>14</sup> At high temperatures, hcp Co is known to undergo a martensitic phase transition to the fcc structure at around 695 K. At still higher temperatures it further undergoes an isostructural phase transition to a paramagnetic phase having a Curie temperature of 1400 K (Ref. 15). At ambient temperatures, the hcp phase has been shown to transform to the fcc phase between 105 and 150 GPa (Ref. 16). The first-principles calculations<sup>15,16</sup> and density and compressibility considerations suggest the high-pressure fcc phase to be nonmagnetic, while the quenched high-temperature fcc phase is expected to be magnetic.<sup>17</sup> Recent impulsive stimulated light scattering and Raman measurements<sup>18</sup> indicated an anomalous density dependence of the aggregate elastic constants and of the  $E_{2g}$  mode Grüneisen parameter at about 60 GPa, well below the pressure of phase transition. Magnetoelastic coupling and a collapse of the magnetic moment were suggested as possible causes for this behavior. A high-pressure study on the metastable fcc structure showed that it fully transforms to the hcp phase by 24 GPa, though the starting pressure of transformation was not determined.<sup>19</sup> Obviously all these studies indicate a rich variety of pressure-induced phenomena in cobalt, encouraging similar studies on the nanocrystalline form of Co. However, to the best of our knowledge, no high-pressure studies have so far been carried out on the nanocrystalline Co and the present study on the encapsulated fcc Co is among the first ones in this category. In this article we present the results of our high-pressure x-ray diffraction experiments on cobalt-filled MWCNTs.

### EXPERIMENTAL DETAILS

Cobalt-filled multiwalled carbon nanotubes were prepared using cobalt nanoclusters as catalysts (generated through ammonia plasma treatment) by microwave plasma chemical vapor deposition technique. High-resolution TEM studies show

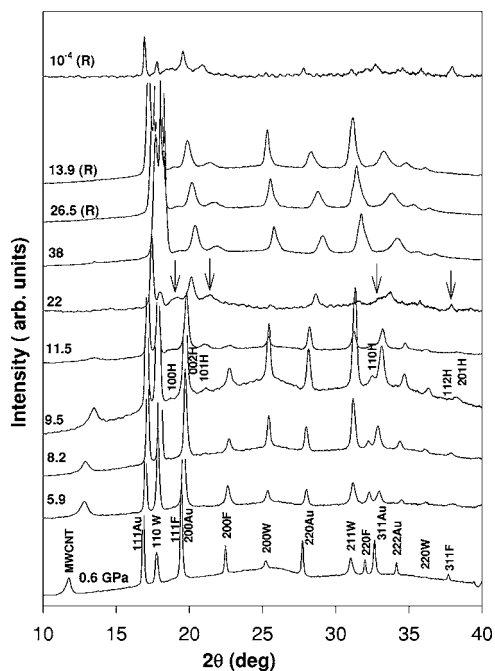


FIG. 1. X-ray diffraction profiles of Co-filled MWCNTs at a few representative pressures. For each profile the corresponding pressure (in GPa) is indicated on the left-hand side. R represents the diffraction profiles with decreasing pressure. The peak marked MWCNT is the characteristic peak of the multiwalled carbon nanotubes associated with the average intershell distance. Indices marked with Au are for gold (pressure calibrant), F for fcc phase, H for hcp phase, and W for tungsten. At 22 GPa, the arrows represent the observed hcp peaks. The diffraction pattern on complete release of pressure shows absence of fcc phase implying the irreversible nature of fcc – hcp transformation.

the presence of perfect single-crystalline nanowires encapsulated inside multiwalled carbon nanotubes. The diameter of the nanowires ranges from 6 to 20 nm and the length varies between 0.29 and 0.9  $\mu\text{m}$ . The (111) planes of face-centered-cubic cobalt are found to be inclined at an angle of  $39.4^\circ$  with respect to the tube axis. More details of the method of preparation and characterization are given in Ref. 13.

For the purpose of high-pressure experiments, cobalt-filled MWCNTs along with a few particles of gold, were loaded in a hole of  $\sim 120 \mu\text{m}$  diam drilled in a preindented  $\sim 70 \mu\text{m}$  tungsten gasket of a Mao-Bell kind of diamond-anvil cell (DAC). Methanol: ethanol: water  $\sim 16:3:1$  mixture was used as pressure-transmitting medium which provides a hydrostatic pressure environment up to  $\sim 15$  GPa. The pressure was determined from the known equation of state of gold.<sup>20</sup> High-pressure angle dispersive x-ray diffraction experiments were carried out up to  $\sim 38$  GPa at the 5.2R (XRD1) beamline of Elettra synchrotron source with monochromatized x rays ( $\lambda=0.69012 \text{ \AA}$ ). The diffraction patterns were recorded using a MAR345 imaging plate detector kept at a distance of  $\sim 21$  cm from the sample. Two-dimensional imaging plate records were transformed to one-dimensional diffraction profiles by the radial integration of diffraction rings using the FIT2D software.<sup>21</sup>

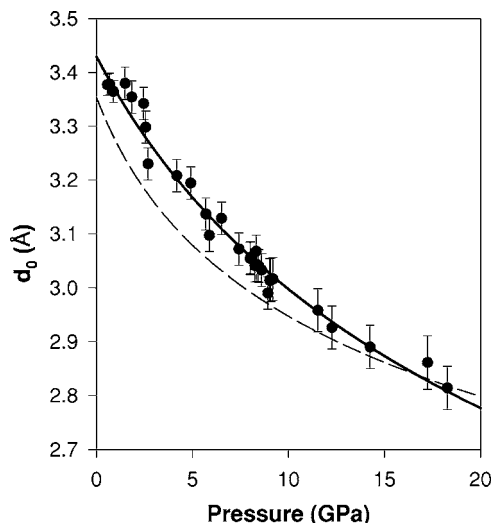


FIG. 2. Variation of the average intershell distance  $d_0$  with pressure. Variation of  $d_{002}$  line of graphite (dashed line) is also plotted for comparison.

## RESULTS AND DISCUSSION

Figure 1 shows the diffraction patterns of Co-filled MWCNTs at a few representative pressures. Before we discuss the behavior of nanocrystalline  $\beta$ -Co, we focus on the results of the MWCNTs. The diffraction peak observed at  $2\theta = 11.73^\circ$  (marked as MWCNT) is the characteristic peak for the multiwall carbon nanotubes representing the average intershell distance. The observed value of average  $d_0$  is  $3.43 \text{ \AA}$  at ambient pressures and compares favorably with the values reported by other investigators.<sup>22</sup> Its difference from  $d_{002}$  of graphite ( $3.353 \text{ \AA}$ ) may be interpreted as due to the curvature of the tubes. The asymmetric line shape of the MWCNTs diffraction peak can be due to a distribution of intershell distances because  $d_0$  is known to decrease with the radii of the tubes.<sup>22</sup> Therefore we identify  $d_0$  with the average intershell separation. The value of  $d_0$  was determined by fitting the asymmetric line shape with a sum of Gaussian and Lorentzian.<sup>23</sup> The variation of this intershell spacing  $d_0$  with pressure is shown in Fig. 2. From the width of the MWCNT Bragg peak and using Scherrer's formula, we estimate the total wall thickness of the MWCNT to be  $\sim 9$  nm which agrees well with the results obtained from TEM (Ref. 13). As shown in Fig. 3, beyond 9 GPa the full width at half maximum (FWHM) of the MWCNT Bragg peak begins increasing, a feature similar to what has been observed for the pristine tubes by us and others.<sup>12,24</sup> This has been ascribed to partial disorder or heterogeneous deformation of the tubes. It should be noted that the observed increase of the FWHM of the MWCNT peak is not due to the nonhydrostatic stresses, as can be inferred from the comparison of the FWHM of the MWCNT peak with that of the gold pressure calibrant, also given in Fig. 3. Moreover, unlike the iron-filled MWCNTs (Ref. 12), no sharp change of the intershell separation was observed in this case. When fitted to the one-dimensional Murnaghan equation,<sup>25</sup> we get  $B=50\pm 3$  GPa and  $B'=5.5\pm 0.7$ , which compares well with our earlier results on iron-filled MWCNTs (Ref. 12). Therefore, we can say that

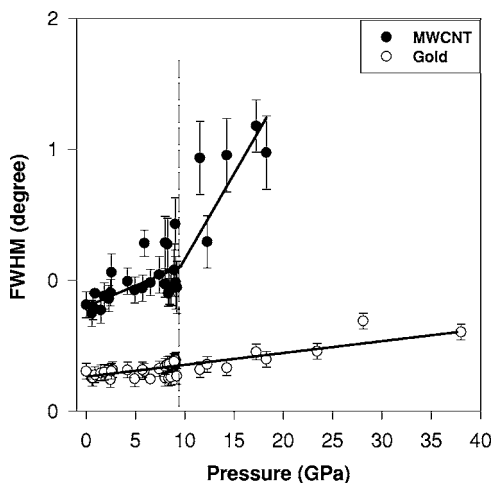


FIG. 3. Variation of the FWHM of the MWCNTs' diffraction line for cobalt-filled MWCNTs. The linewidth for Au (220) is also plotted for comparison. The increase in FWHM of the diffraction peak of MWCNTs is apparent from the solid line drawn as a guide to the eye.

the compressibilities of both iron-filled and cobalt-filled tubes are quite similar. We should also point out that as the intensity of the MWCNT diffraction peak reduces beyond 9 GPa, the errors in  $d_0$  increase beyond this pressure.

At ambient conditions, the diffraction pattern in the  $2\theta$  range of  $15^\circ$ – $40^\circ$ , can be very well analyzed with the help of the Le-Bail profile fitting<sup>26</sup> in terms of three components, viz., fcc Co ( $\beta$  phase), fcc Au (pressure calibrant), and bcc-tungsten (gasket) ( $wR_p=3\%$ ,  $R_p=1.5\%$ ,  $\chi^2=0.16$ ). This is shown in Fig. 4. From the width of the  $\beta$ -Co peak and using Scherrer's formula we get the average diameter of the single-crystalline cobalt nanowire to be  $\sim 10$  nm, which compares well with the TEM results.<sup>13</sup> The refined unit-cell dimension

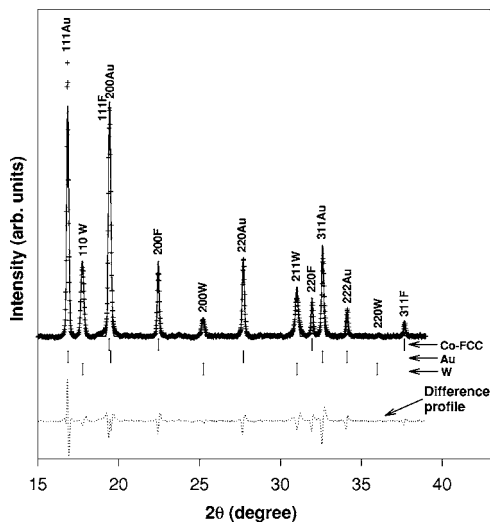


FIG. 4. Le-Bail profile fitting of the diffraction pattern at ambient conditions. The diffraction pattern is fitted with three components (fcc-Co, Au pressure calibrant, and tungsten gasket). Peaks marked with F, Au, and W represent fcc (Co), gold, and tungsten diffraction lines, respectively.

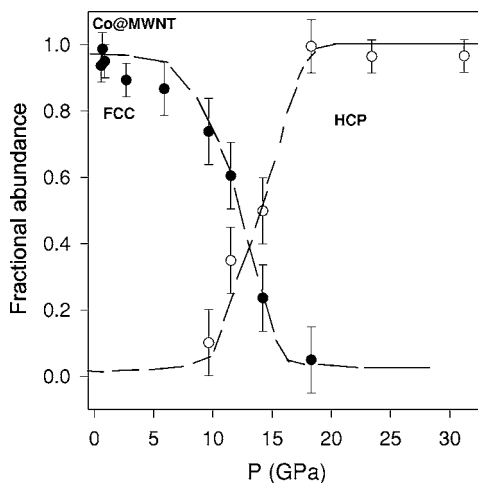


FIG. 5. Variation of fractional abundance of fcc and hcp phases as a function of pressure.

of  $\beta$ -Co (space-group  $Fm3m$ ) is determined to be  $3.544 \pm 0.001 \text{ \AA}$  compared to  $\sim 3.52 \text{ \AA}$  of bulk  $\beta$ -Co (Ref. 19). At a pressure of  $\sim 9$  GPa, fcc cobalt starts transforming irreversibly to the hcp phase. Across the mixed phase region, the relative abundances of the fcc and the hcp phases have been obtained by the comparison of the integrated intensities of the  $(200)_{\text{fcc}}$  and  $(101)_{\text{hcp}}$  peaks [after the normalization of the diffraction patterns with respect to the  $(220)$  diffraction peak of gold]. The variation of abundance of fcc and hcp phases as a function of pressure is shown in Fig. 5. These results show that this transformation is completed by  $\sim 15$  GPa. The lattice parameters of the hcp phase near the transition pressure ( $\sim 9$  GPa) are found to be  $a = 2.455 \pm 0.002 \text{ \AA}$  and  $c = 4.185 \pm 0.003 \text{ \AA}$ , compared to the values of bulk hcp Co at  $\sim 9$  GPa, which are  $a = 2.461 \text{ \AA}$  and  $c = 3.989 \text{ \AA}$  (Ref. 16). The axial ratio  $c/a$  of the hcp phase at 9 GPa is found to be  $\sim 1.7$ , which is much larger than that of the bulk metal, i.e.,  $\sim 1.623$  at ambient conditions.<sup>16,19</sup> Somewhat larger values of lattice parameters of nanocrystalline cobalt (of both phases) compared to bulk are consistent with the general trend in most of the materials and are believed to be due to the larger free surface in nanoparticles.<sup>27</sup> Figure 6 shows the pressure variation of lattice constants of both fcc and hcp phases. Variation of  $c/a$  as a function of pressure is plotted as an inset in Fig. 6. For comparison, the theoretical variations deduced from the first-principles full potential linear-muffin-tin orbital (LMTO) calculations of Yoo *et al.*<sup>16</sup> are also shown. The axial ratio ( $c/a$ ) decreases with pressure and around 27 GPa, the variation of axial ratio becomes similar to the theoretical estimates and is close to the value of the ideal hcp structure.

Pressure-volume behavior of the encapsulated nano-Co is shown in Fig. 7, which shows that the transformation is weakly first order, associated with a volume change of  $\sim 1.2\%$ , consistent with the displacive mechanism available for fcc-hcp transformation.<sup>28</sup> Comparisons of  $V_0$  at ambient conditions ( $V_{0\text{-fcc}} = 11.18 \text{ \AA}^3$ ,  $V_{0\text{-hcp}} = 11.09 \text{ \AA}^3$ —extrapolated for hcp) indicates that hcp may be a slightly denser phase, suggesting fcc to be metastable even when in nanocrystalline form. Theoretical variation of volume with pressure, as given

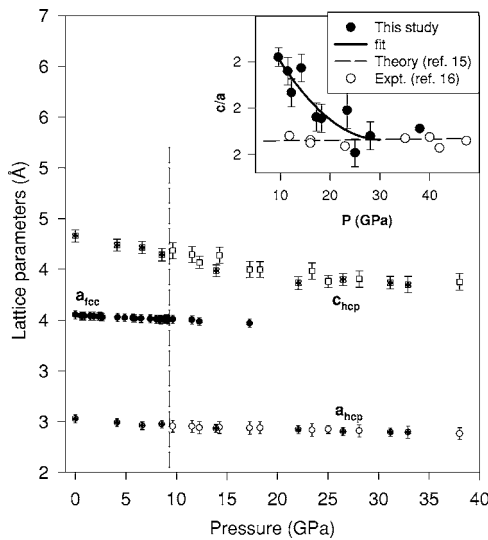


FIG. 6. Variation of lattice parameters for the fcc and hcp phases as a function of pressure. The filled circles represent data for the fcc phase. For the hcp phase, the data on increase of pressure are represented by open symbols (circles for  $a_{\text{hcp}}$  and squares for  $c_{\text{hcp}}$ ) while the corresponding crossed symbols denote data on release of pressure. Variation of  $c/a$  as a function of pressure is plotted as an inset. For this, the filled circles represent the present data and the best fit is shown by the solid line. Experimental results for the hcp phase (bulk), shown as open circles, are from Ref. 16. The dashed flat line represents the theoretical variation of  $c/a$  from Ref. 15.

in Ref. 15, is also shown in this figure. Our results show that beyond  $\sim 15$  GPa for the hcp phase, the experimental variation of volume with pressure is somewhat larger than the theoretical predictions. The comparison for the fcc phase is an extrapolation of the theoretical estimates obtained at higher pressures.<sup>16</sup> The observed pressure variation in this phase is also found to be slightly larger than the theoretical predictions. Fit of experimental P.V. results to the Murnaghan equation of state<sup>25</sup> for the fcc phase gives,  $B = 224 \pm 5$  GPa with  $B' = 3.6 \pm 1$  (for the Vinet equation of state<sup>29</sup>  $B = 223.7 \pm 4$  GPa with  $B' = 3.6 \pm 1$ ). These results are in agreement of the values determined by Yoo *et al.*<sup>16</sup> for the fcc phase observed beyond 105 GPa ( $B = 224$  GPa), differing somewhat from the results of Ref. 19 which gave  $B = 199$  GPa. However, it should be pointed out that the results of Ref. 18 were essentially derived from only one fcc (200) peak and may be limited in accuracy. These results are in contrast with our earlier observations of enhancement in compressibility of the encapsulated nanocrystalline  $\alpha$ -Fe and  $\text{Fe}_3\text{C}$  compared to bulk. For the hcp phase, our experimental results give  $B = 215 \pm 10$  GPa with  $B' = 1.6 \pm 0.4$  (Vinet equation of state gives  $B = 219 \pm 11$  GPa with  $B' = 1$ ), i.e., its bulk modulus is somewhat higher than determined earlier, i.e.,

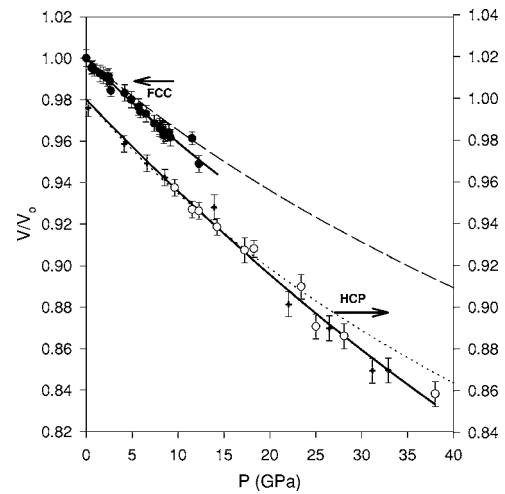


FIG. 7. Variation of  $V/V_0$  as a function of pressure for fcc and hcp phases. Filled circles represent the data for the fcc phase. For the hcp phase, the open circles and cross signs (+) represent data on increase and decrease of pressure, respectively. As the  $V/V_0$  variations for the fcc and hcp phases are too close, these are artificially shifted with respect to each other by representing these on the left and right vertical scales. The solid lines are the fits to the third-order Birch-Murnaghan equation of state. The dotted and dashed lines are the theoretical curves for the fcc and hcp phases, respectively (from Ref. 15; for the fcc phase the curve is an extrapolation to lower pressures).

199 GPa (Ref. 19). The explanation of this behavior needs further experimental work.

In summary, the nanowires of cobalt formed in the MWCNTs, existing in the  $\beta$  (fcc) phase at ambient conditions, undergo an irreversible transformation to the hcp phase at  $\sim 9$  GPa. The irreversibility of the transformation is understandable in terms of metastability of the fcc phase at ambient conditions. In contrast to the iron-filled carbon nanotubes, the cobalt nanowires are not found to be more compressible compared to the bulk. Also unlike Fe-filled tubes, the Co-filled carbon nanotubes do not show any abrupt reduction in intershell separation and show only partial reversible amorphization beyond  $\sim 9$  GPa. This suggests that sudden compaction observed in Fe-filled MWCNTs may be due to the phase transition observed in  $\text{Fe}_3\text{C}$  in that system. In this context, it is interesting to note that recent x-ray magnetic circular dichroism studies indicate that nanoparticles of  $\text{Fe}_3\text{C}$  undergo a high moment to low moment transition around 10 GPa (Ref. 30).

#### ACKNOWLEDGMENTS

We are thankful to E. Bussetto and P. Maurizio for their support during the experiments at XRD1 beamline of Elettra synchrotron. We thank the Department of Science and Technology, Government of India, for financial assistance.

<sup>1</sup>H. Dai, J. H. Hafner, A. G. Rinzler, D. T. Colbert, and R. E. Smalley, *Nature (London)* **384**, 147 (1996).

<sup>2</sup>S. J. Trans, R. M. Veschuereen, and C. Dekker, *Nature (London)* **393**, 49 (1998).

<sup>3</sup>P. G. Collins, A. Zettle, H. Bando, A. Thess, and R. E. Smalley, *Science* **278**, 100 (1997).

<sup>4</sup>W. A. de Heer, A. Chatelain, and D. Ugarte, *Science* **270**, 1179 (1995).

- <sup>5</sup>S. Fan, M. G. Chapline, N. R. Franklin, T. Tomblor, A. M. Cassell, and H. Dai, *Science* **283**, 512 (1999).
- <sup>6</sup>M. A. Burns, B. N. Johnson, S. N. Brahmaandra, K. Handique, J. R. Webster, M. Krishnan, T. S. Sammarco, P. M. Man, D. Jones, D. Hedsinger, C. H. Mastrangelo, and D. T. Burke, *Science* **282**, 484 (1998).
- <sup>7</sup>M. Shim, N. W. S. Kam, R. J. Chen, Y. Li, and H. Dai, *Nano Lett.* **2**, 285 (2002).
- <sup>8</sup>C. N. R. Rao, B. C. Satishkumar, A. Govindaraj, and M. Nath, *New Dir. Tribol., Plenary Invited Pap. World Tribol. Congr., 1st* **2**, 78 (2001).
- <sup>9</sup>M. Monthioux, *Carbon* **40**, 1809 (2002).
- <sup>10</sup>Y. J. Kang, J. Choi, C-Y. Moon, and K. J. Chang, *Phys. Rev. B* **71**, 115441 (2005).
- <sup>11</sup>S. Karmakar, Surinder M. Sharma, M. K. Mukadam, S. M. Yusuf, and A. K. Sood, *J. Appl. Phys.* **97**, 054306 (2005).
- <sup>12</sup>S. Karmakar, Surinder M. Sharma, P. V. Teredesai, and A. K. Sood, *Phys. Rev. B* **69**, 165414 (2004).
- <sup>13</sup>P. K. Tyagi, A. Misra, M. K. Singh, D. S. Misra, J. Ghtak, P. V. Satyam, and F. Le Normand, *Appl. Phys. Lett.* **86**, 253110 (2005).
- <sup>14</sup>J. Sort, N. M. Mateescu, J. Nogues, S. Surinach, and M. D. Baro, *J. Metastable Nanocryst. Mater.* **12**, 126 (2002).
- <sup>15</sup>C. S. Yoo, P. Soderlind, and H. Cynn, *J. Phys.: Condens. Matter* **10**, L311 (1998).
- <sup>16</sup>C. S. Yoo, H. Cynn, P. Soderlind, and V. Iota, *Phys. Rev. Lett.* **84**, 4132 (2000).
- <sup>17</sup>P. M. Marcus and V. L. Moruzzi, *J. Appl. Phys.* **63**, 4045 (1988).
- <sup>18</sup>A. F. Goncharov, J. Crowhurst, and J. M. Zaug, *Phys. Rev. Lett.* **92**, 115502 (2004).
- <sup>19</sup>H. Fujihisa and K. Takemura, *Phys. Rev. B* **54**, 5 (1996).
- <sup>20</sup>D. L. Heinz and R. Jeanloz, *J. Appl. Phys.* **55**, 885 (1984).
- <sup>21</sup>A. P. Hammersley, S. O. Svensson, M. Hanfland, A. N. Fitch, and D. Hauserman, *High Press. Res.* **14**, 235 (1996).
- <sup>22</sup>C. H. Kiang, M. Endo, P. M. Ajayan, G. Dresselhaus, and M. S. Dresselhaus, *Phys. Rev. Lett.* **81**, 1869 (1998).
- <sup>23</sup>D. Louer, in *Powder Diffraction*, edited by S. P. Sen Gupta and P. Chatterjee (Allied, New Delhi, 2002), pp. 1–16.
- <sup>24</sup>C. Liang-Chang, W. Li-Jun, T. Dong-Sheng, X. Si-Shen, and J. Chang-Qing, *Chin. Phys. Lett.* **18**, 577 (2001).
- <sup>25</sup>F. D. Murnaghan, *Proc. Natl. Acad. Sci. U.S.A.* **30**, 244 (1944).
- <sup>26</sup>A. C. Larson and R. B. Von Dreele, *GSAS: General Structure Analysis System* (Los Alamos National Laboratory LAUR Publication, 1998).
- <sup>27</sup>B. Palosz, S. Gierlotka, S. Stel'makh, R. Pielaszele, P. Zinn, M. Winzenick, U. Bismayer, and H. Boysen, *J. Alloys Compd.* **286**, 184 (1999).
- <sup>28</sup>It is well known that the fcc phase can transform martensitically into the hcp phase by a continuous distortion through Shoji–Nishiyama mechanism [Z. Nishiyama, *Martensitic Transformation* (Academic, New York, 1978), p. 49]. Analysis of this mechanism to deduce the free-energy landscape as a function of configuration coordinates is discussed by I. Folkins and M. B. Walker, [*Phys. Rev. Lett.* **65**, 127 (1990)].
- <sup>29</sup>P. Vinet, J. Ferrante, J. Rose, and J. Smith, *J. Geophys. Res.* **92**, 9319 (1987).
- <sup>30</sup>E. Duman, M. Acet, E. F. Wassermann, J. P. Itie, F. Baudelet, O. Mathon, and S. Pascarelli, *Phys. Rev. Lett.* **94**, 075502 (2005).